FRETTING FATIGUE PROBLEMS ASSOCIATED WITH ALMOST FLAT CONTACTS

M.Ciavarella[1], G.Demelio[1] and D.A.Hills[2]

[1]*Dip. di Progettazione e Produzione Industriale, Politecnico di Bari*
Viale Japigia 182, 70126 Bari, ITALY
[2]*Dept. of Engineering Science, Oxford University*
Parks Road, Oxford OX1 3PJ, UK

ABSTRACT: A fretting fatigue pad is simulated as a flat punch having rounded corners. The contact problem is solved under conditions of normal loading and a shearing force, less than that necessary to cause full sliding. Further, the interior stress state induced is found, and it is shown that, unless the corner radius becomes vanishingly small, the stress field in the region of the pad corners is well defined. A crack is then inserted in the region of high tension, and a solution for the crack-tip stress intensity factor found, using the method of distributed dislocations. Thus, a complete solution in mechanics is generated for a nominally flat pad, most often used in fretting fatigue experiments, but having a slightly modified geometry. Finally, issues regarding design against fretting fatigue are discussed: it is concluded that the use of this geometry is generally highly recommended, as a optimum between the Hertzian, and the limit flat geometries. This advantage was not evident from a stress field analysis.

KEYWORDS: Contact Stresses, Flat punch, Fretting Fatigue, Crack initiation, Design

INTRODUCTION

Fretting is an insidious source of damage in many mechanical components and assemblies. Usually a primary source of failure in mechanical components is fatigue. When the presence of fretting is associated with decreased fatigue performance, the effect is known as fretting fatigue. This is a subject drawing equally on materials science and applied mechanics, and has recently received quite a vast interest and effort in many research investigations, both on theoretical and experimental aspects. The areas covered at Oxford in the past few years include: (a) modelling of contact problems under partial slip loading that produces the surface damage; (b) modelling of short cracks by precise, efficient techniques, such as the distributed dislocations method; (c) experimental simulation of fretting fatigue; (d) correlation of data from experiments conducted in (c), together with production of associated growth criteria, and lastly; (e) understanding surface phenomena known critically to influence fretting fatigue, such as surface finish and friction. This paper will concentrate selectively on only some of these aspects, and deals with a contact geometry that has not considered in this context before, although it is of considerable interest in the design of experimental setups, particularly as it is not remote from that usually encountered in practical applications. We start by considering the desirable features to be included in the design of an experimental fretting fatigue test apparatus, and propose using a new pad geometry to overcome some problems. Then, we move on to describe recent work on this geometry of contact problem by the authors

(Ciavarella et al., 1997), in order to collect the key parts of the contact problem solution, with the assumption that the effect of bending on the symmetry of the contact is negligible, and we will then proceed to solve the associated crack problem. This will be done using the distributed dislocation technique (Nowell and Hills, 1987), and calibrations for the stress intensity factors arising given. Finally, the results presented are discussed in a different context, viz. for designing *against* fretting fatigue, where the geometry under consideration provides a reasonable realistic idealization, and represents a very promising alternative to the Hertzian and flat geometries for design purposes.

FRETTING FATIGUE TESTING

Fretting fatigue tests may be designed with two distinct purposes in mind; they may either be used to provide a materials ranking test, to enable a material's resistance to fretting fatigue to be found qualitatively, or they may have the object of attempting to understand the fretting fatigue process in some detail. In the latter case, both initiation and propagation may be quantified, and for a full understanding of each phenomenon it is essential that all the salient variables associated with the contact must be known reliably. This means that we need to know the relative slip displacement between every particle within the contact, together with the surface traction distribution (controlling initiation); and the corresponding internal stress state (controlling propagation). In order to achieve this it is essential that the contact geometry be designed so as to have the following characteristics:

1. The contact should be well-defined, insensitive to minor imperfections in manufacture of the specimen, and insensitive to moderate surface finish changes.
2. The contact pressure distribution, shear traction distribution and partial slip characteristics should be known explicitly.
3. The corresponding internal state of stress should be capable of being determined in a closed form, and there should be no singular point, with attendant plasticity.

These requirements suggest that an incomplete contact, exemplified by the Hertzian geometry, should ideally be used, as all of these objectives have been attained, and indeed much of our recent fretting fatigue experimental work at Oxford has used an apparatus based on this geometry, using either a single hydraulic actuator to apply both the bulk load and fretting force (Bramhall,1973), or a two-actuator machine for better independent control of these two parameters (Hills and Nowell, 1992). There are, however, three features of this type of design which are undesirable, viz.

1. The apparatus is expensive, bulky, and requires hydraulic power.
2. The frequency at which it may be run is very low, as it is limited by the inertia of the pad assembly, so that many tests, particularly in the high-cycle regime, take a long time to complete.
3. The geometry is very remote from that usually encountered in practice, which is usually `complete'. Examples include splined shaft connections, or the dovetail fixings of blades in a jet engine. Now, whilst we maintain that the problem of fretting must be reducible to the salient contact conditions for the tests to be of value, it is also true that it is desirable for the test geometry to resemble the prototype, because, (a) it permits more

of the characteristics of the contact to be reproduced faithfully in the experiment, (b) it means that the *size* of the contact area can be matched to the prototype, and size is known to have a profound influence on fretting fatigue performance (Nowell and Hills,1990), and (c) the degree to which debris entrapment occurs, if fretting wear arises, ought to match the prototype. These criticisms do not arise in the other category of test, used principally for materials work, and which employs a rotating bending configuration (Edwards, 1981), as shown in Figure 1(a).
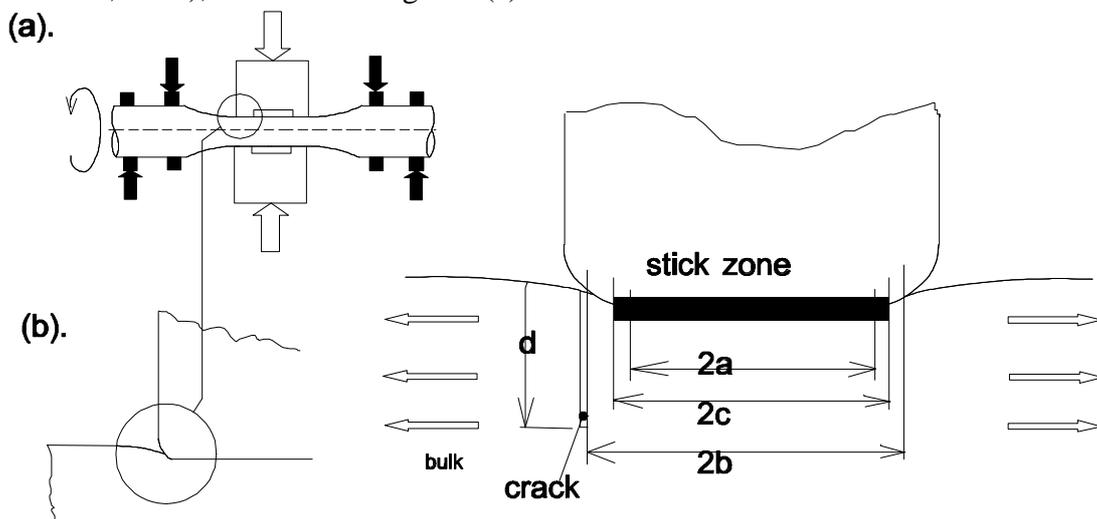

Figure 1 - Rotating bending fretting fatigue setup   Figure 2 - Geometry of the contact

However, the main difficulty with this experimental configuration is that a flat-ended pad is employed on the bridge specimen, and this gives rise to several other difficulties, insofar as the following original objectives are not met;

1. The geometry is hypersensitive to manufacturing errors, and the entrapment of scarf between pad and specimen is also like to change the contact pressure distribution markedly.
2. The contact problem is difficult to solve, and usually requires a resort to intensive use of numerical methods (Sato,1992). Further, the internal stress field generated may again have to be found numerically, and the partial slip characteristics will be difficult to determine.
3. There is an implied singularity at the corner of the specimen, and this will certainly give rise to plasticity, whose extent may prove difficult to determine.

In this paper, we wish to propose a modification of the rotating bending test which meets all the objections normally encountered, giving the best characteristics of each class of experiments. All that is required is the addition of a small radius to the edges of the fretting pads (fig.1(b)). These may readily be added using a numerically controlled machine tool, which must be employed anyway, in order to form the `bridge' shape. The contact and crack problems are then accurately solved, as presented in the following, and therefore the proposed setup presents characteristics that render it attractive in many respects.

CONTACT PROBLEM

The geometry of the fretting pad is shown in Fig.2, and the problem consists of an elastic punch (body 1) pressed onto the rotating-bending specimen, idealised as an elastic half-plane (body 2), which may, in general, be elastically dissimilar. The straight part of the punch boundary is of length a and the corners are of radius R. The form of the latter will be approximated by parabola, in the same way that they are in the Hertz problem. The contact force, P, is applied through the centre of the pad, and the extent of the ensuing contact is b. For the pad to be realistically represented by a half-plane, and further, for the radius to be capable of being represented by a parabola, the contact zone must not extend too far towards the extreme edges of the pad, i.e. (b-a)<<R.

Details of the solution of the contact problem are given in (Ciavarella et al., 1997), and we shall here restrict ourselves to summarising the basic results. First, the coordinate, x, is transformed into a new variable, φ, by

$$x = a \frac{\sin \varphi}{\sin \varphi_0} \tag{1}$$

where φ_0 is related to the size of the contact, b, by

$$\sin \varphi_0 = \frac{a}{b}. \tag{2}$$

The actual contact size is then implicitly given by

$$\frac{PAR}{a^2} = \frac{\varphi - 2\varphi_0}{2 \sin \varphi_0} - \cot \varphi_0 \tag{3}$$

and the contact pressure distribution is

$$\frac{b p(\varphi)}{P} = -\frac{2/\pi}{\varphi - 2\varphi_0 - \sin 2\varphi_0} \left[(\varphi - 2\varphi_0)\cos\varphi + \ln\left(\left| \frac{\sin(\varphi + \varphi_0)}{\sin(\varphi - \varphi_0)} \right|^{\sin\varphi} \left| \tan\frac{\varphi + \varphi_0}{2} \tan\frac{\varphi - \varphi_0}{2} \right|^{\sin\varphi_0} \right) \right] \tag{4}$$

It may be noted, in particular, that the pressure at the straight/curved transition point is finite, due to the continuity assumed in the profile, as the two logarithmic terms cancel each other.

PARTIAL SLIP CONTACT: LOADING

With the contact law established we now turn our attention to the partial slip problem. We shall assume that a harmonically varying shearing force, Q, is applied, starting from zero and increasing monotonically, while P is held fixed.

We will consider the shear tractions arising in the contact, q(x), as a superposition of the full sliding one, fp(x), with a *difference* part, q'(x). Thus

$$q(x) = fp(x) + q'(x), \qquad |x| \le c$$
$$q(x) = 0, \qquad |x| > c \tag{5}$$

It may be shown (see Edwards,1981 again, or Sato, 1992 for a general treatment of plane partial slip problems) that the position of the stick/slip interface, c, must always lie in the radius part of the punch, i.e. a<c<b and that the corrective traction, q'(φ), is given by

$$\frac{cq'(\phi)}{fP} = -\frac{2/\pi}{\pi - 2\phi_0 - \sin 2\phi_0}\left[(\pi - 2\phi_0)\cos\phi + \ln\left(\left|\frac{\sin(\phi + \phi_0)}{\sin(\phi - \phi_0)}\right|^{\sin\phi}\left|\tan\frac{\phi + \phi_0}{2}\tan\frac{\phi - \phi_0}{2}\right|^{\sin\phi_0}\right)\right] \quad (6)$$

where

$$x = a\frac{\sin\phi}{\sin\phi_0} \quad (7)$$

and is related to the size of the stick zone by

$$\sin\phi_0 = \frac{a}{c} \quad (8)$$

The actual stick zone size, c, is related to the value of the dimensionless shearing force by

$$\frac{Q}{fP} = 1 - \left(\frac{c}{b}\right)^2\frac{\pi - 2\phi_0 - 2\sin\phi_0}{\pi - 2\phi_0 - 2\sin\phi_0}, \qquad \frac{c}{b} > \frac{a}{b}, \qquad \frac{Q}{fP} < 1 \quad (9)$$

and when c/b>a/b, Q/fP=1, so that the slip zone migrates inwards along the curved parts of the boundary, as the shearing force is increased, and just reaches the straight part of the boundary at the point of incipient sliding.

PARTIAL SLIP CONTACT: UNLOADING & CYCLIC LOADING

It is important, under a cyclically varying shearing force, to be able to track the position of the stick-slip interface and the value of the shearing traction distribution along the contact throughout each loading cycle. In the previous section we gave the result for the first quarter cycle of loading, when the shearing force is being increased monotonically. Let us now assume that the maximum shearing force, Q_{max}, has been attained, producing a stick zone of dimension c_{max}, and the shearing force is being reduced. Upon decreasing Q by an infinitesimal amount, the requirement that in each slip zone the shear stress is in the same direction as the slip *increment* is violated, and hence instantaneously stick envelopes the entire contact patch. As the shearing force is decreased by a finite amount reverse slip develops, starting from the outer edges of the contact, where the pressure falls continuously to zero. Details of the calculation itself are contained in the papers cited (Ciavarella et al., 1997, Ciavarella, 1997), and here we shall be content with recording the salient results. A region of counter-slip must form, and grow inwards. The shear stress distribution is the superposition of the partial slip solution previously obtained, together with a reverse full sliding component (to model correctly the reverse slip in the new slip zones) and a new corrective part q''(x) in the new stick zone of dimension $\tilde{c}$ presently unknown, as

$$q(x) = fp(x) + q'(x) - 2fp(x) + q''(x), \qquad |x| \le c$$
$$q'(x) = 0, \qquad |x| > c_{max} \qquad\qquad (10)$$
$$q''(x) = 0, \qquad |x| > \tilde{c}$$

At a shearing force Q on the falling shear stress curve therefore, the size, $\tilde{c}$, of the stick zone at any instant is given implicitly by

$$\frac{Q}{fP} = -1 + \left(\frac{\tilde{c}}{b}\right)^2 \frac{2(p - 2\psi_0 - 2\sin\psi_0) - \left(\frac{c_{max}}{\tilde{c}}\right)^2 (p - 2f_0 - 2\sin f_0)}{p - 2j_0 - 2\sin j_0}, \qquad (11)$$

and

$$\sin f_0 = \frac{a}{c_{max}}, \qquad \sin \psi_0 = \frac{a}{\tilde{c}}. \qquad (12)$$

whilst the shearing traction distribution is obtained using the second correction

$$\frac{\tilde{c} q''(j)}{fP} = \frac{4/p}{p - 2\psi_0 - \sin 2\psi_0} \left[(p - 2\psi_0)\cos\psi + \ln\left(\left|\frac{\sin(\psi + \psi_0)}{\sin(\psi - \psi_0)}\right|^{|\sin\psi|} \left|\tan\frac{\psi + \psi_0}{2} \tan\frac{\psi - \psi_0}{2}\right|^{|\sin\psi_0|}\right)\right] \quad (13)$$

where

$$x = a\frac{\sin\psi}{\sin\psi_0} \qquad (14)$$

When the shearing force has decreased to Q=-Q$_{max}$, the partial slip configuration is perfectly reversed, and a new cycle would start, perfectly symmetrical with the last one. It is clear then that cyclic loading is completely determined by these equations.

INTERIOR STRESS FIELD

A knowledge of the contact pressure and shear traction distributions, together with the stick zone size, is a useful start in analysing this class of contact in relation to fretting fatigue problems, but more information is needed if the crack initiation and propagation conditions are to be quantified in a comprehensive way. Specifically, we needed to know the complete internal stress field, and the surface relative displacement within the stick zone. It is clear from the results in the previous section that all that is needed is the stress state corresponding to normal pressure and full sliding shearing tractions, as the influence of a partial slip shear distribution can be found by superposition and appropriate scaling. A Muskhelishvili potential approach is appropriate, expanding the traction distribution as a series in terms of Chebyshev polynomials of second kind U(x) as

$$p(x) = -\sqrt{1 - x^2} \sum_{n=0}^{\infty} b_n U_{2n}(x) \qquad (15)$$

In full sliding the normal and shear tractions are related by q(x)=fp(x) throughout the whole contact, and Mushkelishvili's potential is (8)

$$\Phi(z) = \frac{1-if}{2pi}\int_{-1}^{1}\frac{p(t)dt}{t-z} = -\frac{i+f}{2}\sum_{n=0}^{\infty}b_n R_{2n+1}(z) \tag{16}$$

where dimensionless coordinates are now adopted for x, y, t, z=x+iy, by normalizing them with respect to the contact half-width b. The function R is given by $R_{2n+1}(z) = \left(z - \sqrt{z^2-1}\right)^n$, and for the definition of the branch cut of the square root function see (Gladwell,1980). No simple closed-form expression for the coefficients, b_n, is possible. From the potential, the stresses as well as the displacement derivatives can be obtained from the standard relations

$$\frac{S_x + S_y}{2} = 2\,\mathrm{Re}\,\Phi(z)$$

$$\frac{S_y - S_x + 2it}{2} = \left(\bar{z} - z\right)\Phi'(z) - \overline{\Phi}(z) - \Phi(z) \tag{17}$$

$$2m\left(\frac{\P u}{\P x} + i\frac{\P v}{\P y}\right) = \left(\bar{z} - z\right)\overline{\Phi}'(z) - \Phi(\bar{z}) + k\Phi(z)$$

where κ is the Kolosov' constant, equal to 3-4ν in plane strain, ν being Poisson's ratio. The absolute displacements may be found only to within an arbitrary constant, which is a characteristic of plane elasticity. However, of particular interest in this case is the value of the surface tangential displacement within the slip zones, as this gives a measure of the amount of damage, and is needed to evaluate the energy density expended at each point in working against friction. Further, the relative slip displacement must be zero within the stick zone, and hence we are able to write the absolute displacement down, by integrating the strains parallel to the surface.

CRACK PROBLEM

Experience with a number of related crack/contact problems (Munisamy et al., 1995) has shown them to be uncoupled, in the sense that the presence of the crack has a negligible influence on the contact pressure distribution, even for very long cracks adjacent to the contact patch itself, when the stress intensity factor becomes insensitive to the exact pressure distribution, in any case. This result enables us to split up the crack and contact elements, and hence to solve them as two separate problems. We may therefore take the internal stress field derived above, and use it as one of the sub-problems in an exploitation of Bueckner's theorem (Bueckner., 19581). The approach which will be followed is to use the method of distributed dislocations to clear the line of the crack of tractions, and to infer the crack tip stress intensity factors from the dislocation density at the crack tip (Nowell and Hills,1987). The first step in the solution is therefore to derive the stress state induced by a single dislocation, present at a general point in the half-plane. This is well-known (Nowell and Hills,1987), and is conveniently written in the form

$$S_{iy}(x) = \frac{m}{p(1+k)}K(x,x)b_i(x), \qquad i = x, y \tag{18}$$

where $b_i(\xi)$ is the magnitude of the Burgers vector of the dislocation, in direction i, positioned at ξ, μ is the modulus of rigidity. The function $K(x, \xi)$ is given explicitly in (Nowell and Hills,1987), and will not be reproduced here; it consists of a Cauchy singular term, together with a bounded part which represents the influence of the presence of the free surface. As the applied shearing force, Q, is taken through a cycle the crack faces will be pressed together when the shearing force is directed towards the crack, and pulled apart when it is directed away. The crack will extend when the mode I stress intensity factor reaches a maximum value, and the material ahead of the crack tip will suffer little damage when the crack tip is closed. We shall therefore concentrate our attention on the case when $Q \Rightarrow Q_{max}$, and, if the corresponding stress along the line x=-d is given by $\hat{s}_{iy}(x)$, the requirement that the crack faces be traction-free is given by

$$0 = \hat{s}_{iy}(x) + \frac{m}{p(1+k)} \int_{crack} K(x,x)B_i(x), \qquad i = x, y \qquad (19)$$

where $B_i(\xi)$ is the dislocation density, given by

$$B_i(x) = \frac{\P}{\P x}b_i(x), \qquad i = x, y \qquad (20)$$

This integral equation may be normalised over the interval [-1,1] and is then a standard singular integral equation with a generalized Cauchy kernel, which may be reduced to a family of algebraic equations using standard procedures (Nowell and Hills,1987)., and the crack tip stress intensity factors, K_I, K_{II} found.

RESULTS

Contact Stress Field

This has been described earlier, but it is worth drawing out some further features. The first is that there is a maximum normal load which we may apply if the idealization of the radiused portion of the punch is effectively to be represented by a parabola. In practice this part of the calculation may need to be used in an inverse way: the maximum contact pressure (either over the central portion or over the slip zones) may be decided, either to represent the contact pressure present in the prototype, or to avoid yield (Ciavarella et al., 1997), and the minimum acceptable radius determined. Figure 3 shows the pressure distribution for a/b equal to 0, 0.25, 0.5, 0.75,1, i.e. ranging from the Hertzian case, to the limit flat profile case (here we consider the rigid punch solution).
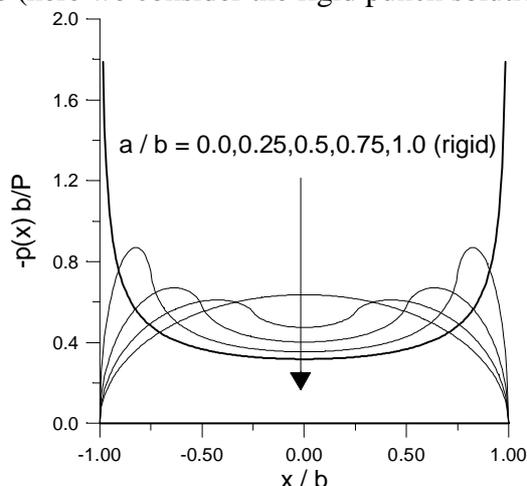

Figure 3 - Pressure distribution for rounded edge flat punch, for geometric ratio a/b=0.0, 0.25, 0.5, 0.75, 1.0. The bold line is for the limit rigid flat punch solution.

Then, in Figure 4, the maximum pressure p_{max} is given as a function of the ratio a/b, which tends to infinity as the a/b tends to 1 (i.e. the radius R becomes vanishingly small), and to the Hertzian value as a/b decreases. It is clear that, for design purposes, it is convinient to remain in the rage, say, a/b<0.7, if we want to avoid the pressure to be so high that surface damage is very fast.
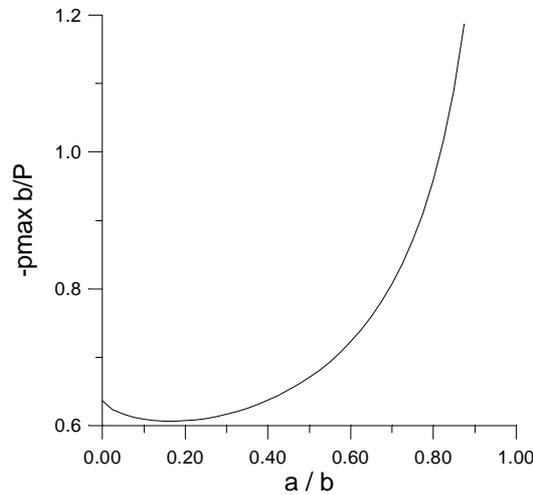

Figure 4 - Maximum pressure for rounded edge flat punch, as a function of the geometric ratio a/b=0.0, 0.25, 0.5, 0.75, 1.0.

Another interesting property of the contact is the relationship between the ratio Q/fP, representing the dimensionless tangential load, and the size of the stick zone, c/b, and this is given in Figure 5. It is evident that, as the pad becomes close to the limit flat punch, the configuration approaches the limiting behaviour of full/stick -full/slip, observed in the flat punch. In this limiting case, stick persists everywhere, until the ratio Q/fP becomes unity, and then slip occurs for the whole of the contact area. This features means that it will important to control the value of Q/fP imposed carefully, by using a displacement control (as, indeed, it is in a rotating bending test), to avoid moving into the sliding regime, with consequent gross movement of the contact patch.
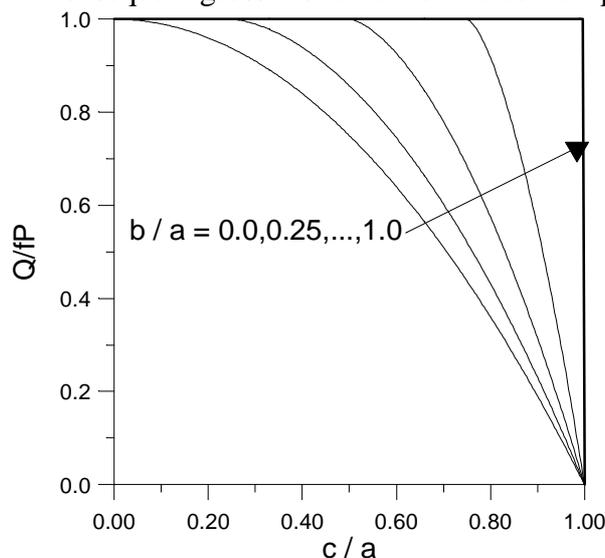

Figure 5 - Dimensionless tangential load parameter Q/fP, as a function of stick area size c/a. Geometric ratio a/b=0.0, 0.25, 0.5, 0.75, 1.0.

The next variable to be considered is the relative tangential slip displacement of surface particles, within the slip zones. We may also note that the surface density of frictional energy dissipated may be found as the product $\delta(x)\tau(x)$. This gives an indication of the most probable site of crack initiation, although it should also be borne in mind that the surface tension $\sigma_{xx}(x)$ also plays a key role in the early development of a crack. It is not clear yet how these functions combine to produce a reliable criterion for crack initiation, as it is known that this process is very influenced by other material characteristics: in particular surface roughness and grain size may play an important role, comparable in significance with the details of the elastic solution, in terms of the idealised smooth geometry of the contact. For these reasons, and as the parameters involved for a complete representation of these quantities in the partial slip regime depend on a number of independent parameters (friction coefficient f, ratio Q/fP, ratio a/b, bulk stress σ_{bulk}) no results are given in a graphical form here.
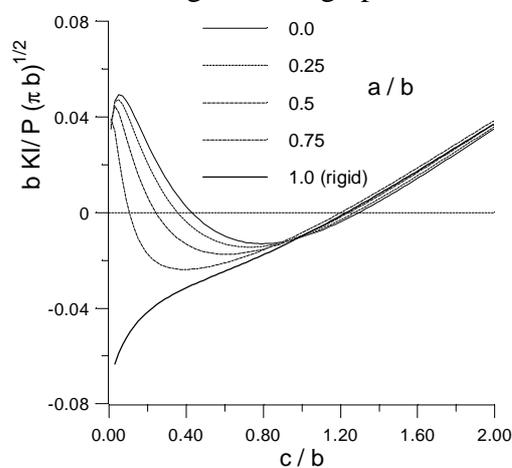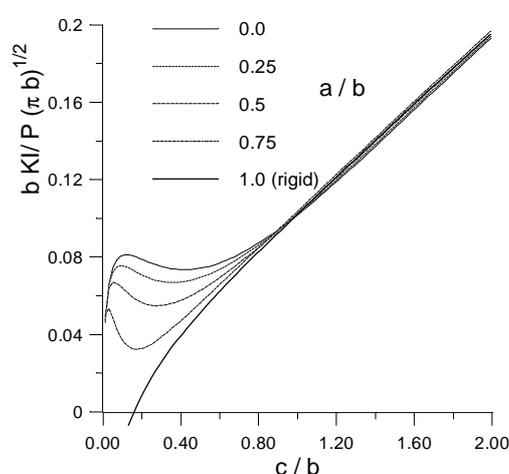

Figure 6

Figure 7 - As in Figure 6, except $b/P\varsigma_{bulk} =0.2$.

Figure 6 - Non dimensionalized mode I stress intensity factor for crack at the trailing edge of the contact, perpendicular to the surface. Geometric ratio a/b=0.0, 0.25, 0.5, 0.75, 1.0. Q/fP=0.4, f=0.4, $b/P\varsigma_{bulk} =0.1$. Negative factors plotted only for comparison.

Crack Tip Stress Intensity Factors

If crack initiation and early development is controlled by the surface contact stress/displacement conditions, then *propagation* must clearly be controlled by the stress intensity factors, and these quantities may be found reliably, if the crack dimension is large enough, compared to the average grain size of the material. Figure 6 gives the mode I stress intensity factor for a particular (but typical) set of parameters, namely Q/fP=0.4, f=0.4, $b/P\sigma_{bulk}$=0.1, for different shapes of the punch, i.e. a/b=0.0, 0.25, 0.5, 0.75, 1. It is worth remarking that the shape of punch profile affects the first region of propagation, c/b<0.4, very significantly, as for the flat punch (a/b=1) the implied value of K_I is very negative from the outset until a large size of the crack is reached, whereas for a Hertzian pad (a/b=0) the crack is initially open. This is obviously due to the difference in the contact stress field which is very different for the two conditions, and results in a different behaviour of the initial stage of propagation; specifically, under a flat punch the crack can grow only in mode II, although the high compressive stress between the crack faces means that the nett shear stress available to cause mode II loading is likely to be

small. Experimentally, it is usually observed that, if cracks grows at all under such conditions, they are inclined of about of about 45 degree, until some point is reached where they meet the grain boundary. If the crack has reached a sufficient length for K_I for a *normal* crack now to be positive, it will tend to curve and continue to grow perpendicular to the surface.

By contrast, under a Hertzian contact, we can expect the crack to grow be capable of growing perpendicular to the surface at a much earlier stage, although self-arrest is clearly a serious problem and could occur anywhere in the range $0.4<c/b<1.2$. In the intermediate range of punch profiles ($0.25<a/b<0.75$ in the figure), the behaviour implied lies somewhere between these two extremes. It is interesting to note that, for the particular range of parameters employed in Figure 6, the normalised crack length at which K_I becomes greater than zero is substantially independent of the punch profile; the principal difference between the profiles therefore lies in their intrinsic behaviour in propelling very short cracks. The conclusion we can draw is that the smaller the pad radius, the larger the bulk tension needed to cause a crack to start, and indeed, the greater the depth to which this tension must persist in order to propel the crack over possible self-arrest conditions. Figure 7 shows a similar set of results to those given in Figure 6, but with double the bulk tension, $b/P\sigma_{bulk}=0.2$, and it is seen that for most geometries the crack tip experiences a monotonically increasing stress intensity factor, and that, with the exception of the flat-ended punch, the opening mode stress intensity is always positive. Therefore, notwithstanding the range of configuration does not cover all possible parameter values, and does not consider inclined crack, and the influence of K_{II}, the results show a strong indication that the use of a almost flat pad with the proposed geometry is beneficial against the fretting fatigue crack propagation. Of course, this effect has to be considered together with the maximum allowable value of pressure, for which Figure 4 gives indications.

Crack arrest: designing against fretting fatigue

The principal import of this paper is to propose a new kind of geometry for fretting fatigue test pads which, we believe, will combine the advantages of the two kinds of tests widely in use today. One of the features now included is a realism between the characteristic of the contact and those found frequently in engineering practice, and hence this attribute means that we can also use the results found to infer desirable features of *real* contacts so as to inhibit fretting fatigue.

First, as we have noticed in the last paragraph, there are conditions under which a crack self-arrests. We may seek to make use of this event in order to ensure a safe design, although it should be emphasised that such a design strategy is only feasible if the bulk tension is reliably known, and is small. Also, the chances of employing the approach are much greater when the contact is complete or almost complete, than when it is near Hertzian.

Secondly, we note that plain fatigue and fretting fatigue differ substantially in two respects: (a) the initiation of fretting cracks is due to surface damage produced by relative movement, whereas in plain fatigue cracks usually develop only from pre-existing defects, or localised plasticity; (b) the fretting crack initiates from a known region at the free surface. Therefore, although a much better understanding of several aspects of fretting fatigue is still needed, and in particular in the parameters controlling surface damage and crack initiation, it is clear that the proposed geometry can be

recommended as a design possibility, as a particular optimum between the Hertzian, and the limit flat geometry. The real optimum is clearly dependent on actual loading conditions and materials properties

CONCLUSION

The contact problem for a flat punch with rounded corners has been solved, together with a proper formulation for crack propagating from the trailing edge of the contact area in partial slip conditions, providing the base for both (i) future testing equipments using pad of this geometry; (ii) designing against fretting fatigue for typical mechanical components.

REFERENCES

Bramhall, R., 1973, "Studies in fretting fatigue", D.Phil. Thesis, University of Oxford.

Bueckner., H.F., 1958,"The propagations of cracks and the energy of elastic deformation" , *Trans.ASME*, 80, 1225-1230, (1958).

Ciavarella, M. , Hills, D.A., Monno., G. ,1997, "The Influence of rounded edges on indentation by a flat punch.", *J. Mech. Engng. Sci.*, under review.

Edwards, P.R.,1981, "The application of Fracture Mechanics to predicting fretting fatigue", *Fretting Fatigue*, ed. R.B. Waterhouse, Applied Science publishers, London, pp.67-98.

Gladwell, G.M.L.,1980, "Contact problems in the classical theory of elasticity", Sijthoff & Noordhoff,, Alphen aaa Olen Rijn.

Hills,D.A. and Nowell,D.,1992, "The development of a fretting fatigue experiment with well-defined characteristics", *ASTM STP 1159 Standardization of Fretting Fatigue Test Methods and Equipment* ASTM, Baltimore, MD, USA, pp.69-84

M. Ciavarella, 1997, "The generalized Cattaneo partial slip plane contact problem", *Int. J. Solids Struct.*, under review.

Munisamy,R.L., Hills,D.A., and Nowell,D., 1995, "An analysis of coupling between plane contacts and cracks", *Euro. J. Mech, part A: Solids*, 14, 1, pp. 985-991.

Nowell, D. and Hills, D.A., 1990,"Crack initiation criteria in fretting fatigue", *Wear*, 136, pp. 329-343.

Nowell, D. and Hills, D.A.1987, "Open cracks at or near free edges", *J. Strain Anal.*, 22, 3,pp. 177-185.

Sato, K., 1992, "Determination and Control of Contact Pressure distribution in Fretting Fatigue", *ASTM STP 1159 Standardization of Fretting Fatigue Test Methods and Equipment* ASTM, Baltimore, MD, USA, pp.85-100.